Poly(L-lactide-*co*-glycolide) Microporous Membranes for Medical Applications Produced with the Use of Polyethylene Glycol as a Pore Former

Malgorzata Krok, Elzbieta Pamula

Department of Biomaterials, Faculty of Materials Science and Ceramics, AGH – University of Science and Technology, Krakow 30-059, Poland

Received 13 July 2011; accepted 22 December 2011
DOI 10.1002/app.36697
Published online in Wiley Online Library (wileyonlinelibrary.com).

ABSTRACT: The aim of this study was to prepare microporous poly(L-lactide-*co*-glycolide) (PLGA) membranes by mixing PLGA previously dissolved in methylene chloride with polyethylene glycol (PEG) as a pore former. PEGs with different molecular weights of 300, 400, 600, 1000, and 3400 kDa were used. The PEG concentration was fixed at 20–80%, resulting in membranes with increased porosity. The properties of the membranes were characterized by tensile testing, and by SEM, AFM, and FTIR. Solvent evaporation rate from PEG/PLGA blends and PEG solutions was also estimated. Cytocompatibility of the materials in contact with osteoblast-like MG 63 cells was studied and cell viability and morphology were assessed. SEM evaluation demonstrated that porosity of the membranes can be easily controlled by addition of a defined amount of PEG. The membranes produced with 60% PEG have the most favorable mechanical properties from the point of view of medical applications: tensile strength of 12.6 ± 2.3 MPa, Young's modulus of 0.53 ± 0.08 GPa, and total elongation at break of 56.4% ± 12.3%. The size and distribution of pores in the membranes depend on PEG molecular weight: low-molecular weight PEG resulted in more homogenous distribution of pores, while high-molecular weight PEG resulted in asymmetric membranes with the skin on the air-cured surface. The obtained membranes support cell growth and are promising materials for biological applications. © 2012 Wiley Periodicals, Inc. J Appl Polym Sci 000: 000–000, 2012

Key words: poly(L-lactide-*co*-glycolide); polyethylene glycol; phase separation; guided tissue regeneration

INTRODUCTION

Membranes are one of the most important forms of materials used in medicine. They are used in drug delivery systems, artificial organs, tissue regeneration, diagnostic devices, as coatings on medical devices, and in bioseparations.[1,2] The membranes are also applied in periodontology, in so called guided tissue regeneration (GTR) to protect bony defects from invasion of connective tissue and mucous membrane, and assure adequate conditions for regeneration of bone tissue.[3] Different biologically stable polymers (e.g., expanded polytetrafluoroethylene and polyethylene terephtalate) or biodegradable materials (e.g., collagen, poly-ε-caprolactone, polylactides, polyglycolide, copolymers of lactide and glycolide—PLGA, and chitosan) have been processed into membranes for the GTR technique.[3–8]

PLGA belongs to a group of bioresorbable aliphatic polyesters and it is commonly used in medical applications to produce surgical sutures, bone fracture fixation elements and fibrous GTR membranes for periodontology.[9] In recent times, PLGA has been used to create scaffolds for bone tissue engineering.[10] A key feature of PLGA is its degradation by hydrolysis. The final degradation products of PLGA, i.e., lactic and glycolic acids, are metabolized through the Krebs cycle to water and carbon dioxide. Because of this there is no necessity of a second surgery to remove the medical devices produced from PLGA.[11] Another key advantage of PL GA in comparison with homopolymers of lactide or glycolide is the possibility of simple copolymerization of different molar fractions of lactide and glycolide to adapt its mechanical properties, kinetics of hydrolytic degradation and properties important from the point of view of polymers processability.[12,13]

The membranes can be prepared by a conventional liquid–liquid demixing process, a freeze-gelation method,[14] an in-air drying phase inversion technique,[15] electrospinning,[16] or by a fiber-bonding technique.[17] Another method is the phase separation process.[18] The phase separation process is popular

Correspondence to: E. Pamula (epamula@agh.edu.pl).

Contract grant sponsor: The Polish Ministry of Science and Higher Education; contract grant number: N N507 280736.

Contract grant sponsor: The National Centre for Research and Development; contract grant number: N N507 234640.

for membranes or preparation of other porous structures because of simplicity and cost efficiency. Moreover, it is possible to change the pore size and pore density depending on the type of polymer, porogen, and solvent.[19] Phase separation methods were used to produce membranes of polystyrene, cellulose, poly(ε-caprolactone), or nylon-12.[19–23] Nakane et al.[24] and Tsuji et al.[25] fabricated porous poly(L-lactide) membranes with the use of PEG as a porogen. Microporous poly(ε-caprolactone) films obtained with the use of PEG were also manufactured by a solvent-casting-leaching method.[26] More recently microporous poly(L-lactic acid) membranes were produced by PEG solvent-cast/particulate leaching and they were tested as potential scaffolds for bioartificial lacrimal gland device.[27] However, to our best knowledge this is the first study describing methods of fabrication, properties, proposed mechanism of formation, and cell affinity of the nonfibrous PLGA membranes produced with the use of PEG as a pore former.

The principal goal of this study was to prepare barrier, nonfibrous PLGA membranes and to assess their structure and properties interesting from the point of view of medical use, especially the GTR technique. More specifically, we aimed to determine the optimum concentration of PEG in PLGA/PEG blends assuring the highest porosity, favorable mechanical properties and handling of the resulting PLGA membranes. Moreover, we wanted to explore the effect of PEG molecular weight on pore size and pore distribution within the PLGA membranes to control microstructure of the resulting membranes better. In addition, we wanted to gain a deeper insight into the mechanism of phase separation and blend formation in the PEG/PLGA system. As a final point, we wanted to prove cytocompatibility of membranes produced in contact with cells interesting from the point of view of medical use. To this end several membranes of gradual porosity produced with PEG of different molecular weight and concentration were evaluated.

MATERIALS AND METHODS

Materials

The membranes were made from PLGA of molecular weight M_n = 100 kDa, polydispersion index 2.1, molar ratio of L-lactide to glycolide 85 : 15 and density 1.24 g/cm^3. The PLGA was synthesised by in bulk by ring-opening polymerization with the use of low-toxic zirconium compound $Zr(acac)_4$ as an initiator according to a method described previously.[28] As a pore former, PEGs (Aldrich, Germany) with different molecular weights and properties were used: PEG 300 (M_n = 300 kDa, ρ = 1.125 g/cm^3, T_m = −15–−8°C), PEG 400 (M_n = 400 kDa, ρ = 1.128 g/cm^3, T_m = 4–8°C), PEG 600 (M_n = 600 kDa, ρ = 1.128 g/cm^3, T_m = 20–25°C), PEG 1000 (M_n = 1000 kDa, ρ = 1.101 g/mL, T_m = 39°C), and PEG 3400 (M_n = 3400 kDa, ρ = 1.204 g/mL, T_m = 54–58°C). As a solvent for PLGA and PEG methylene chloride (POCh, Gliwice, Poland) was used.

Porous membrane preparation

PLGA and 20, 40, 60, 70, or 80% weight fraction of different PEGs (PEG 300, PEG 400, PEG 600, PEG 1000, or PEG 3400) were codissolved at a concentration of 10% wt/vol in methylene chloride by stirring in a magnetic stirrer for 5 h. After homogenization the mixtures were slip-casted on glass Petri dishes and dried subsequently in air and in vacuum for 24 h and 72 h, respectively. Then the PLGA/PEG blends were immersed in ultra-high quality water (UHQ-water, PureLab, Elga) for 5 days to leach out PEG. Water was exchanged several times a day to ensure PEG leaching out. Detailed method of membrane preparation is described in a submitted patent application.[29] As a reference PLGA film without PEG was also prepared.

Methods of membranes characterization

Tensile test

Tensile testing of the PLGA membranes was conducted with universal testing machine Zwick 1435 (Germany). The test speed was 100 mm/min with 0.1 N preload, specimen length of 40 mm and specimen width of 5 mm. Six samples originating from each type of the membranes (20, 40, and 60% of PEG 400) and PLGA foil were tested. The results are shown as mean ± S.E.M. (standard error of the mean).

Scanning electron microscopy

Scanning electron microscopy (SEM, Nova NanoSEM, FEI) was used for the evaluation of the membrane microstructure. The microphotographs were taken under two magnifications of 2000× and 5000× and an accelerating voltage of 18 kV. Before the analysis, the samples were sputter-coated with a thin carbon layer to make them conductive. The analysis was performed for both membrane surfaces (top surface, i.e., air-cured, and bottom surface, i.e., glass-cured) as well as cross-sections, prepared by breaking the membranes after their immersion in liquid nitrogen.

Atomic force microscopy

The atomic force microscope (Explorer, Veeco) was used to study membrane topography, arithmetic

mean roughness (R_a) and mean diameter of the pores. For both surfaces of the membranes six pictures were registered in contact mode at a scan area of 100 μm × 100 μm and speed of acquisition of 3 lines/s.

Percentage of PEG leached out

The percentage of PEG leached from the membrane was calculated based on the weight difference of the PLGA/PEG blend and that PLGA membrane after the leaching out process. Ten individual membranes (9 cm in diameter) of each type were measured. The results are shown as mean ± S.E.M.

Thickness

The thickness of each membrane was measured by micrometer screw in 10 places and the results are shown as mean ± S.E.M. Membranes with a thickness of 50 μm were expected to be obtained.

Solvent evaporation

The solvent evaporation rates from PEG, PLGA, and PLGA/PEG (60%) solutions in methylene chloride were measured. The solution was poured into a glass petri dish placed on an electronic balance under a fume hood at ambient laboratory conditions (22°C, humidity 60%). The weight change was recorded every minute up to 60 min and then every 5 min up to 120 min. The drying rate was calculated from the slope of the weighing curve for different periods of time (1st period 2–10 min, 2nd period 30–50 min, and 3rd period of 100–120 min) taking into account the surface area of the Petri dish; and it was expressed in $g/cm^2 \cdot s$. The samples were weighed once again after 24 h to determine the mass of remaining solvent.

FTIR spectroscopy

PLGA membranes, PLGA/PEG blends, PEG, and reference PLGA film surfaces were analysed with FTIR spectroscopy (Digilab FTS 60V, Bio-Rad). A method of attenuated total reflection (ATR) was applied using ZnSe as a measuring crystal in the range of 550–4000 cm^{-1} with a resolution of 4 cm^{-1}.

Biological experiment

For cell culture studies, the samples were washed in 70% ethanol, rinsed in sterile PBS, sterilized with UV radiation (20 min on each side), fixed in special inserts to prevent them floating (CellCrown, Scaffdex, Finland), and placed in 24-well plates (Nunclon, Denmark). Two types of membranes were selected for the biological experiment. These were obtained by using 60% PEG 300 and PEG 1000. Cells were seeded on both sides of the membranes (top surface, i.e., air-cured and bottom surface, i.e., glass-cured). PLGA foils and tissue culture polystyrene (TCPS, i.e., bottom of the well plates) were used as controls. Initial cell density was 1.6×10^4 cells per sample (0.8 cm^2). MG 63 osteoblast-like cells (European Collection of Cell Cultures, Salisbury, UK) were cultured on the studied materials in DMEM supplemented with 10% FBS, 1% penicilin/streptomicin, 2 m*M* L-glutamine at 37°C under 5.0% CO_2 atmosphere for 5 days.

Cell viability (MTT test) was measured by the reduction of the tetrazolium salt MTT (3-[4,5-dimethylthiazol-2-yl]-2,5-diphenyltetrazolium bromide) to formazan. MTT solution (5 mg/mL) was added to the wells with cells, after 3 h the reaction was stopped with isopropanol/HCl (0.04*M*), and the optical density of the blue dye was determined at 570 nm using a Multiscan FC Microplate Photometer (Thermo Scientific).[30] The results were expressed as mean ± S.E.M.

Morphology of the cells was observed by fluorescence microscopy (Zeiss Axiovert 40, Carl Zeiss, Germany). The cultured cells were fixed in 4% paraformaldehyde for 1 h, washed in PBS, and stained with acridine orange solution (1 mg/mL) before microscopic examination.

Statistics

The results are shown as mean ± S.E.M. (standard error of the mean). Statistical analysis was performed using the unpaired *t*-test. Significant differences were assumed at $*P < 0.05$; $**P < 0.01$; $***P < 0.001$.

RESULTS

Properties of the membranes produced with different percentage of PEG 400

Gross morphology

Figure 1 presents gross morphology of PLGA membranes produced with different concentration of PEG 400. It is apparent that when using lower concentrations of PEG (up to 60%) it is possible to obtain membranes which are homogenous at the macroscopic level [Fig. 1(A–C)]. The membranes produced with 70% PEG [Fig. 1(D)] and 80% PEG (data not presented) are heterogeneous.

SEM

SEM results of top (air-cured), bottom (glass-cured), and cross-sections through the membranes produced with different concentrations of PEG 400 are

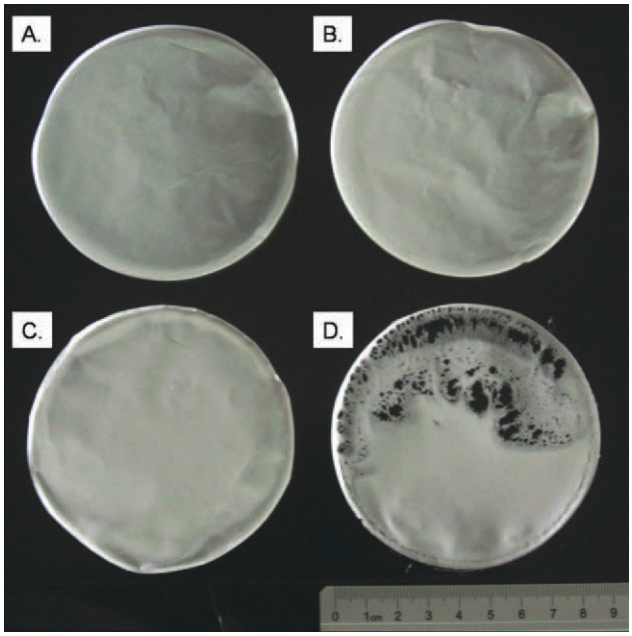

Figure 1 Gross morphology of PLGA membranes produced using different concentrations of PEG 400: A, 20%; B, 40%; C, 60%; and D, 70%. [Color figure can be viewed in the online issue, which is available at wileyonlinelibrary.com.]

displayed in Figure 2. The results show that in the membranes volume fraction of pores depends on PEG concentration being the highest for 60% PEG [Fig. 2(G–I)]. It was also found that the air-cured surface is always less porous than the glass-cured surface [Fig. 2(A vs. B, D vs. E, G vs. H)]. It is worth noting that in the cross-section size of pores increases from top to bottom, especially in the case of 60 and 80% PEG [Fig. 2(I,L)]. For 80% PEG spherical PLGA particles are visible on the membrane surface [Fig. 2(J,K)].

Tensile test

Mechanical properties of PLGA foil and PLGA membranes obtained with different concentration of PEG 400 were evaluated. The results show that tensile strength (R_m), Young's modulus (E), and maximal elongation ($\varepsilon_{F_{max}}$) of the membranes decrease with increasing PEG concentrations while total elongation at break ($\varepsilon_{F_{total}}$) increases (Table I). Figure 3 shows the representative strength/strain curves of reference PLGA foil and PLGA membranes obtained with 20, 40 and 60% of PEG 400. The membranes produced with the highest PEG concentration are the most flexible, have the lowest Young's modulus, and the lowest strength.

Properties of the membranes produced with PEG of different molecular weight

SEM

Figure 4 shows SEM pictures of the membranes produced with 60% PEG differing in molecular weights. This concentration of PEG resulted in production of highly porous membranes with defined, reproducible microstructure and the most optimal mechanical properties from the point of view of medical applications, e.g., flexibility (see Fig. 2, Table I).

The membranes have asymmetric microstructures and their morphology and size of pores depend on PEG molecular weight (Fig. 4). The porosity on the top side decreases with increasing PEG molecular weight. In the membranes produced with PEG 600, 1000, and 3400 nonporous skin is observed [Fig. 4(G,J,M)]. In all the membranes the pores on the bottom are bigger than on the top surfaces. In the case of the membranes obtained with the use of PEG 400, 600, and 1000 [Fig. 4(E,H,J)] the pores on the bottom are less circular and have irregular shapes, which is not the case for the PEG 300 membrane [Fig. 4(B)]. The cross-sections through the membranes demonstrated that the pores are present in the whole volume of the membranes and they are interconnected. The pores have a larger diameter on the bottom side than on the top side; this is especially well visible in the case of the membrane obtained with the use of PEG 1000 [Fig. 4(L)]. The membranes produced with PEG 3400 have different microstructure: on the bottom surface irregular small pores are present [Fig. 4(M–O)].

AFM

AFM pictures of the membranes (Fig. 5) show similar morphologies to those observed in SEM (Fig. 4). Image analysis of AFM pictures enabled mean roughness and mean diameter of pores to be measured on the top and bottom surfaces of the membranes; the results are summarized in Table II. The results show that the pore size on the top surface of the membranes produced with PEG 300 and PEG 400 is $\sim$ 3 μm, while on the bottom surface the size of pores increased from $\sim$ 3 to $\sim$ 20 μm when PEG molecular weight increased from 300 to 1000 Da. On the top surface, the mean roughness decreased from $\sim$ 500 to $\sim$ 180 nm when PEG molecular weight increased from 300 to 1000 Da. Interestingly, for all the membranes the roughness of the bottom surface was always higher than that of the top surface. The membrane obtained with the use of PEG 3400 was not porous on the top and bottom surfaces and it had a considerably different structure as compared to the other membranes.

Thickness and percentage of PEG leached out

The detailed results of thickness and PEG leach out percentage of the membranes are presented in Table II. The thickness of all the membranes was controlled at the level of $\sim$ 50 μm. The percentage of

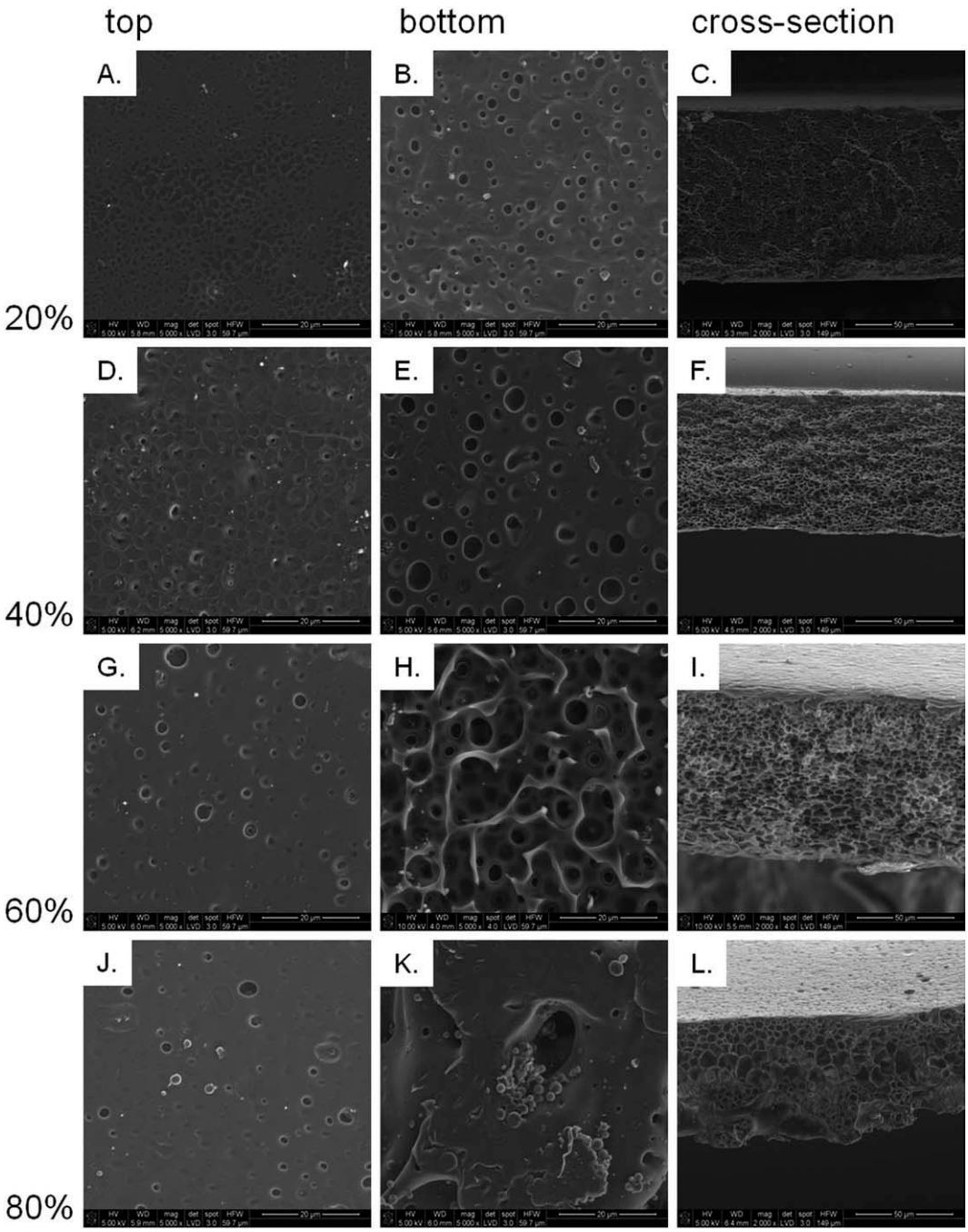

Figure 2 SEM microphotographs of PLGA membranes obtained with different concentrations of PEG 400: 20% (A,B,C), 40% (D,E,F), 60% (G,H,I), and 80% (J,K,L); top surface (A,D,G,J), bottom surface (B,E,H,K), and cross-section (C,F,I,L).

PEG leached out was more than 59% in all cases, except for PEG 3400 and PEG 400. The results show that the thickness as well as percentage of PEG leached out were similar for all the membranes.

Phase separation in PLGA/PEG/solvent system and mechanism of blend creation

Solvent evaporation

Figure 6 presents solvent evaporation curves from PEGs of various molecular weight. The results show that the higher evaporation rate was measured for PEG of the highest molecular weight, i.e., 3400 Da, while the lowest evaporation rate was measured for PEG of the lowest molecular weight, i.e., 300 Da.

The morphology of the resulting PEG films is shown in the upper right hand corner of Figure 6. It is apparent that PEGs of lower molecular weight, e.g., 300, 400, and 600 Da are liquid and transparent, while those of PEG of higher molecular weight, e.g., 1000 and 3400 Da exhibit a typical crystalline spherulitic structure. The size of spherulites in PEG 1000 is higher than that of PEG 3400.

TABLE I
Mechanical Properties of PLGA Foil and PLGA Membranes (mPLGA) Obtained with Different Concentration of PEG 400

	R_m (MPa)	E (GPa)	εF_{max} (%)	εF_{total} (%)
PLGA	52.1 ± 1.5	1.96 ± 0.14	3.49 ± 0.20	4.2 ± 0.3
mPLGA_20% PEG 400	30.2 ± 2.4***	1.48 ± 0.15*	3.54 ± 0.21	9.1 ± 1.2**
mPLGA_40% PEG 400	19.9 ± 1.9***	1.10 ± 0.07***	2.32 ± 0.15**	21.1 ± 6.1*
mPLGA_60% PEG 400	12.6 ± 0.9***	0.53 ± 0.03***	1.97 ± 0.10***	56.4 ± 5.0***

Tensile strength (R_m), Young's modulus (E), maximal elongation (εF_{max}), total elongation at break (εF_{total}). Data are expressed as mean ± S.E.M. Asterisks indicate a statistical significance from the control PLGA group:
* $P < 0.05$;
** $P < 0.01$;
*** $P < 0.001$.

Table III presents solvent evaporation rate and mass of remaining solvent in PLGA/PEG blends. In the first period (2–10 min), the evaporation is fast and it seems to be independent of PEG molecular weight. In the second period (30–50 min), the evaporation rate is more than two orders of magnitude lower and for all samples except that containing PEG 3400 it increases with PEG molecular weight. The same tendency is visible for the third period (100–120 min); however, the evaporation rate is another order of magnitude lower than in the second period. Mass of the solvent remaining in the blends calculated as a difference in mass after drying for 120 min and 24 h was the highest for the blends produced with PEG 300 and decreased when molecular weight of PEG increased. Interestingly, the solvent evaporated very fast from pure PLGA solution (not containing PEG); as a result the mass of PLGA reference foil measured 120 min after casting was the same as after 24 h (data not presented).

FTIR-ATR

Figure 7 shows FTIR-ATR spectra of PEG 1000, PLGA/PEG blend, PLGA membrane, and reference PLGA film.

In the spectra of PEG characteristic bands are visible: stretching vibrations of hydroxyl groups (~ 3400 cm^{-1}), stretching (~ 2860 cm^{-1}) and deformational (in the range 1450–1240 cm^{-1}) vibrations of hydrocarbon in —CH_2 groups, stretching vibrations of C—O and C—O—C groups (in the range 1000–1200 cm^{-1}). Moreover, at lower wavenumbers in the range of 840–940 cm^{-1} bands assigned to bending vibrations of hydrocarbon groups in —CH_2 are observed.[31]

In the spectra of the reference PLGA foil and the PLGA membrane characteristic bands are visible: stretching vibrations of C=O (1746 cm^{-1}), stretching (~ 2860 cm^{-1}) and deformational (in the range 1450–1240 cm^{-1}) vibrations of hydrocarbon in —CH_3 and —CH_2 groups, stretching vibrations of C—O and C—O—C groups (in the range 1000–1200 cm^{-1}).[32] Moreover, in the range of 840–940 cm^{-1} bands assigned to bending vibrations of hydrocarbon groups in —CH_3 and —CH_2 are observed; however, their intensity is much lower than those of PEG.

In the spectra of the PLGA/PEG blend all bands already observed for PLGA and PEG are visible, suggesting that there is no chemical reaction between PLGA and PEG.

Biological evaluation of PLGA membranes

Cell viability

Figure 8 presents MG 63 cell viability evaluated by MTT assay on PLGA membranes produced with the use of PEG 300 and 1000, and reference samples (PLGA foil and TCPS) after 5 days of culture. The results show that cell growth on the top surface of PLGA membranes is the same or significantly higher than on control TCPS. The cell growth on the bottom surface of the membranes is however significantly lower.

Cell morphology

Figure 9 presents morphology and distribution of MG 63 cells cultured on both sides (top and bottom)

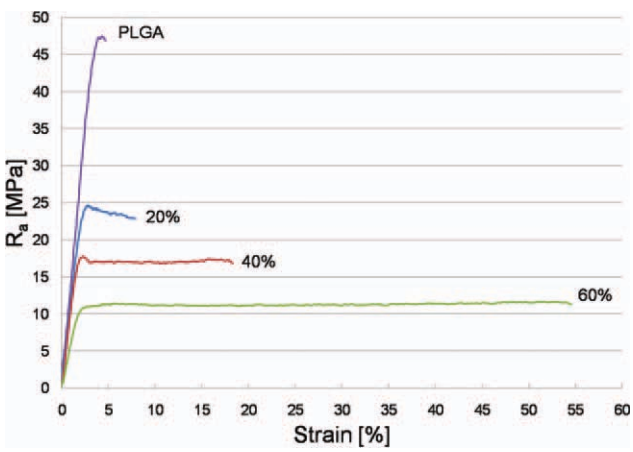

Figure 3 Representative tensile test curves of PLGA foil and PLGA membranes obtained using different concentration of PEG 400. [Color figure can be viewed in the online issue, which is available at wileyonlinelibrary.com.]

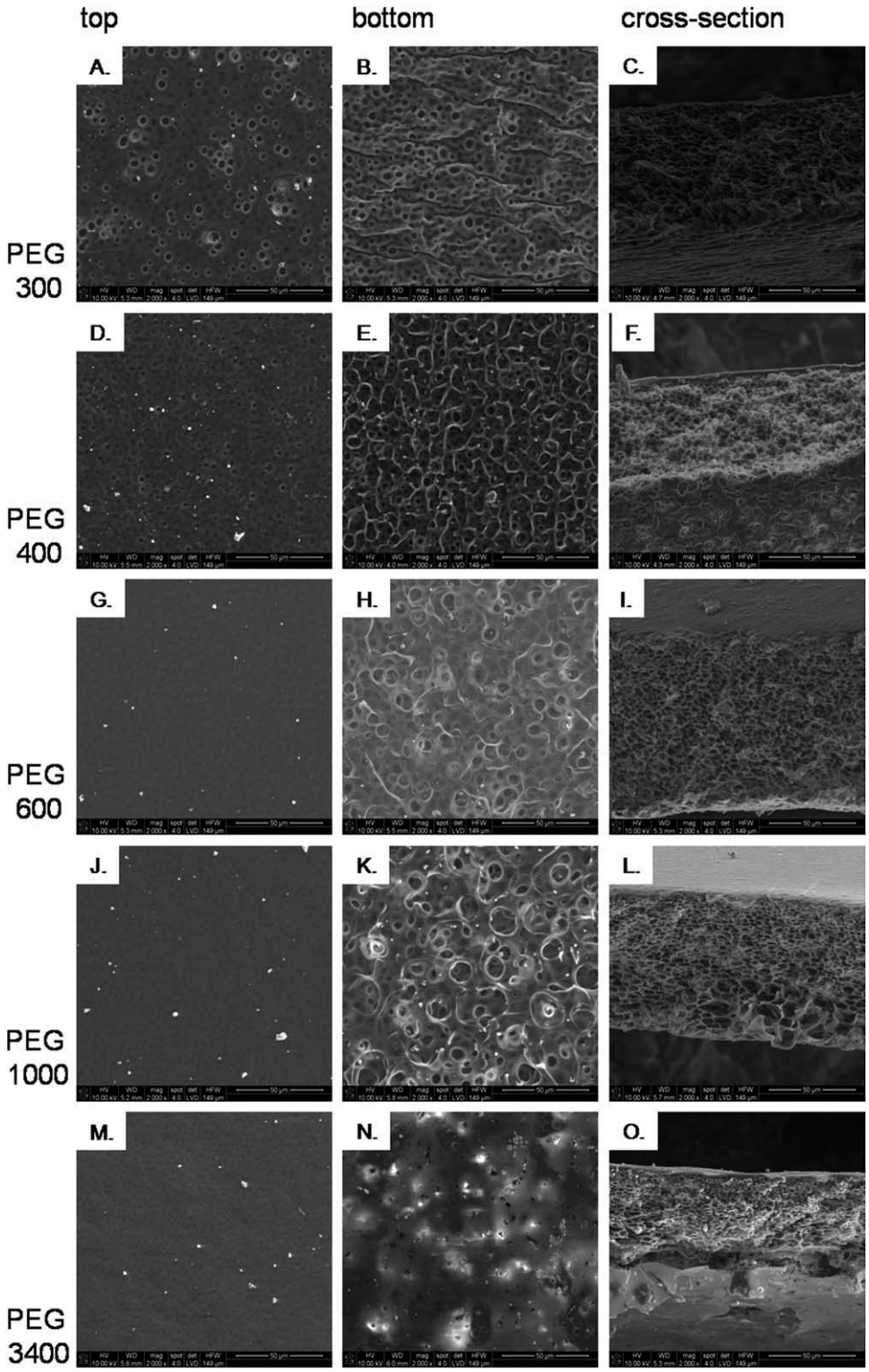

Figure 4 SEM microphotographs of PLGA membranes obtained with the use of 60% PEG 300 (A,B,C), PEG 400 (D,E,F), PEG 600 (G,H,I), and PEG 1000 (J,K,L); PEG 3400 (M,N,O); top surface (A,D,G,J,M), bottom surface (B,E,H,K,N), and cross-section (C,F,I,L,O).

of the PLGA membranes obtained with the use of two types of PEG (300 and 1000 Da) as well as on reference PLGA foil and TCPS. The cells were well spread, polygonal, or spindle-shaped and their morphology was similar to that on control TCPS or PLGA foil. Interestingly, on flat TCPS [Fig. 9(F)], PLGA foil [Fig. 9(E)] and the top surface of the membranes [Fig. 9(A,C)] the cells were

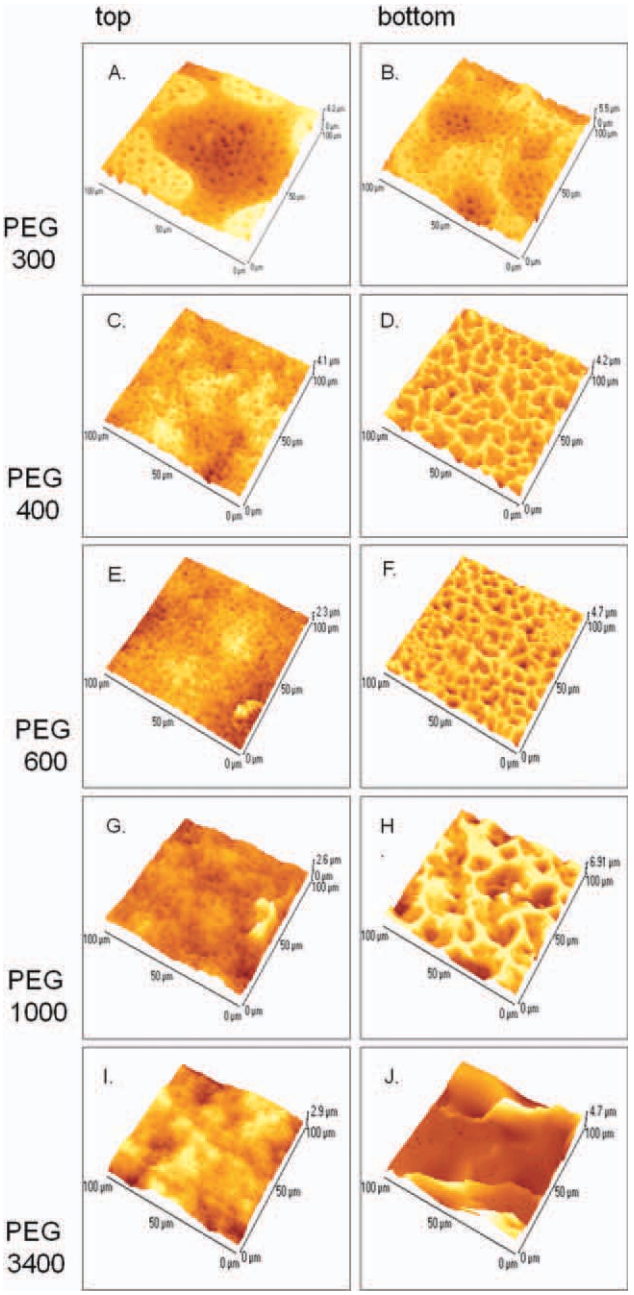

Figure 5 AFM pictures of PLGA membranes obtained with the use of 60% PEG 300 (A,B), PEG 400 (C,D), PEG 600 (E,F), PEG 1000 (G,H); PEG 3400 (I,J); top surface (A,C,E,G,I) and bottom surface (B,D,F,H,J). [Color figure can be viewed in the online issue, which is available at wileyonlinelibrary.com.]

homogenously distributed. On the other hand, on bottom surfaces [Fig. 9(B,D)], i.e., which are more rough and porous, the cells grew in aggregates.

DISCUSSION

As stated in the introduction, the aim of this study was to manufacture PLGA membranes for medical applications (especially for GTR technique) and (i) determine the optimum concentration of PEG in PLGA/PEG blends providing the highest porosity and favorable mechanical properties of the resulting membranes; (ii) explore the influence of PEG molecular weight on pore size and pore distribution within the membranes; (iii) gain deeper insight into the mechanism of phase separation and blend formation in the PEG/PLGA system; and finally (iv) verify if materials produced are compatible with osteoblast-like cells *in vitro*.

Controlling membranes' porosity and mechanical properties

In this study, several PLGA membranes produced by leaching out PEG from PLGA/PEG blends containing different amounts of PEG 400 were analysed. As expected it was found that higher amount of PEG resulted in higher porosity. If the amount of PEG was 70% or more, the membranes were inhomogeneous at macroscopic level because of creation of large phase-separated PEG domains (see Fig. 1).

It was found that tensile properties of the membranes strongly depended on concentration of PEG used as a pore former: the highest PEG concentration, the highest elongation at break, and the lowest Young's modulus were measured. The membranes produced with the use of 60% PEG exhibited tensile properties which were the most promising from the point of view of GTR technique: they were the least brittle, the most flexible and had acceptable strength (see Fig. 3, Table I). The results of mechanical properties obtained in this study are similar to those reported in the literature for different types of newly produced GTR membranes.[4,8,33–35]

The cross-sections through the membranes showed that for 20 and 40% PEG the pores were homogenously distributed within the volume of the material, while for 60–80% of PEG the size of pores exhibited higher polydispersion. This phenomenon can be explained in the following way: when concentration of PEG is low it forms small isolated droplets within the PLGA continuous matrix due to spontaneous phase separation. This spontaneous phase separation is a consequence of higher PLGA solubility in methylene chloride compared to PEG. Although methylene chloride is a good solvent for both PLGA and PEG, Hildebrand solubility parameters of PLGA ($\delta = 21.7$ MPa$^{0.5}$)[36] and methylene chloride ($\delta = 20.2$ MPa$^{0.5}$)[37] are more close to each other than to PEG 400 ($\delta = 23.1$ MPa$^{0.5}$).[37] Another point is that surface free energies of PLGA and PEG are different, because PEG is much more polar than PLGA. When adding PEG to a solution of PLGA in a nonpolar solvent such as methylene chloride, the

TABLE II
Thickness, Percentage of PEG Leached Out, Porosity, Roughness of the PLGA Membranes (mPLGA) Obtained with PEGs Differing in Molecular Weight (mean ± S.E.M.)

Membrane	Thickness (μm)	PEG leach out (% wt)	Pore size (μm)		R_a (nm)	
			Top	Bottom	Top	Bottom
mPLGA_60% PEG 300	50 ± 1	59.2 ± 0.2	3.5 ± 0.3	3.7 ± 0.4	505 ± 18	733 ± 86
mPLGA_60% PEG 400	52 ± 2	58.9 ± 0.4	2.6 ± 0.2	12.5 ± 1.9	391 ± 5	457 ± 29
mPLGA_60% PEG 600	51 ± 1	59.6 ± 0.5	nd	15.3 ± 2.8	236 ± 7	575 ± 4
mPLGA_60% PEG 1000	50 ± 2	59.0 ± 0.2	nd	21.1 ± 3.5	184 ± 4	1186 ± 38
mPLGA_60% PEG 3400	49 ± 2	57.0 ± 0.2	nd	nd	304 ± 62	877 ± 255

nd, not detectable.

PEG phase spontaneously separates forming spherical domains within PLGA matrix, to diminish the surface free energy on the PGLA-PEG interface. This explanation has already been proposed for a poly-ε-caprolactone/PEG system.[26]

When concentration of PEG was high, e.g., above 70%, the PEG phase became continuous and PLGA formed isolated domains, so after leaching out PEG the membranes were heterogeneous. Spherical PLGA particles could be observed on the air-cured surface of the membranes, proving that in some places PLGA domains were embedded in continuous PEG phase [see Fig. 2(K)].

For all the membranes differing in PEG 400 concentration (see Fig. 2), the pores were smaller on the top surface but bigger on the bottom surface. It is most likely due to three phenomena: inhomogeneous evaporation process of the solvent from PLGA and PEG solutions, coalescence of PEG-rich domains and their sedimentation in course of drying. In our studies, it was found that solvent evaporated very fast from the PLGA solution, and after 120 min no changes in mass of the resulting PLGA foil were detected. On the other hand, from PEG 400/PLGA solutions solvent evaporated much more slowly (see Table II, last column). These differences in solvent evaporation rates resulted in the fact that on the air-cured surface dominated PLGA and skin-like morphology was observed in the membrane, while on the glass-cured surface PEG domains in the blend were dominating. When PEG concentration was higher, e.g., 60% or more, higher number of PEG-rich domains had the possibility to collide and agglomerate resulting in lower number of domains but

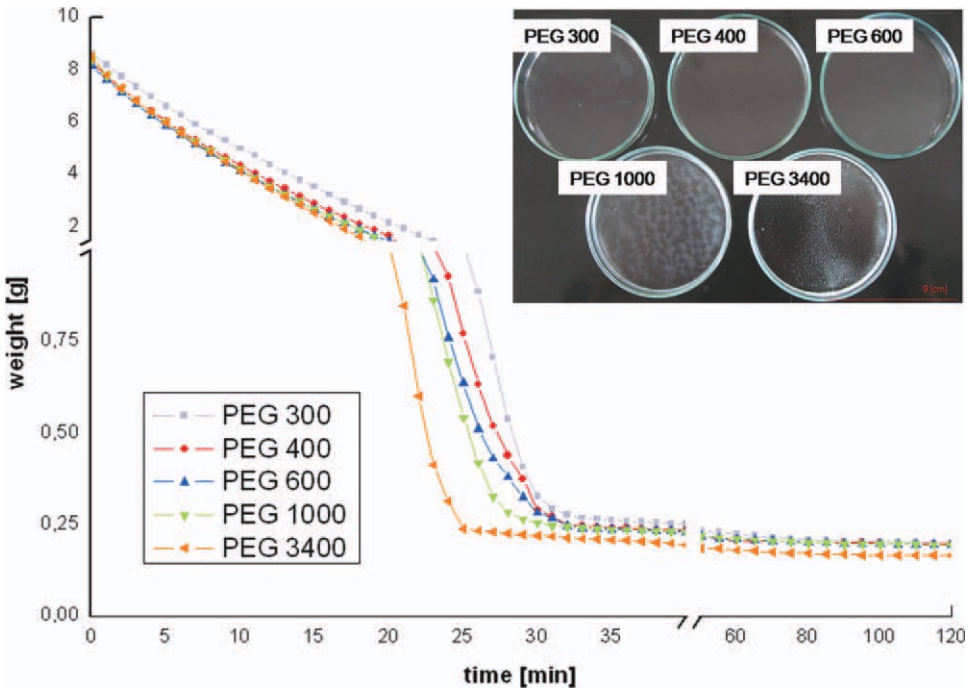

Figure 6 Solvent evaporation from different PEGs: ■ PEG 300, ● PEG 400, ▲PEG 600, ▼ PEG 1000, ▶PEG 3400; insert shows gross morphology of the PEG films after solvent evaporation. [Color figure can be viewed in the online issue, which is available at wileyonlinelibrary.com.]

TABLE III
Solvent Evaporation Rate and Remaining Solvent in PLGA/PEG Blends

Blend	1st period ($g/cm^2 \cdot s$) 2 ÷ 10 (min)	2nd period ($g/cm^2 \cdot s$) 30 ÷ 50 (min)	3th period ($g/cm^2 \cdot s$) 100 ÷ 120 (min)	Remaining solvent mg[a]	Remaining solvent %[b]
bPLGA_60%PEG 300	9.9×10^{-5}	4.8×10^{-7}	0.17×10^{-7}	55	0.75
bPLGA_60%PEG 400	9.7×10^{-5}	6.1×10^{-7}	0.31×10^{-7}	24	0.32
bPLGA_60%PEG 600	9.5×10^{-5}	7.2×10^{-7}	0.58×10^{-7}	22	0.29
bPLGA_60%PEG 1000	9.9×10^{-5}	8.4×10^{-7}	0.73×10^{-7}	21	0.27
bPLGA_60%PEG 3400	9.8×10^{-5}	7.1×10^{-7}	0.73×10^{-7}	21	0.27

[a] Difference in mass after drying PLGA/PEG blends for 120 min and 24 h.
[b] Difference in mass after drying for 120 min and 24 h related to initial mass of the solvent in the PLGA/PEG solution.

of bigger size. Our observation is in agreement with Kamide's theory on particle growth during membrane formation.[38,39] The PEG-rich domains sediment resulting in their preferable accumulation near the surface of glass Petri dish.

Our proposed mechanism of membranes' formation with the use of smaller (20%) and higher (60%) concentrations of PEG 400 is shown in Figure 10(A,B), respectively. For membranes produced with 20% of PEG 400, small isolated PEG-rich domains were dispersed in the PLGA matrix. Because solvent evaporated faster from the PLGA-rich phase than from PEG-rich domains, and drying proceeded from the surface towards inside the film, PEG-rich domains become embedded in the PLGA matrix. After leaching out PEG, the resulting membrane had small pores of size ~ 1 μm homogenously distributed in the whole volume of the membrane [see Fig. 10(A)].

For membranes produced with 60% of PEG 400, a higher number of PEG-rich domains were dispersed in the PLGA matrix, as compared to when the concentration of PEG was 20% [Fig. 10(B)]. In the beginning of the drying, some of the PEG-rich domains in the surface/subsurface regions remained trapped within the PLGA matrix. As drying proceeded, PEG-rich domains inside the film started to coalesce and descend to the bottom of the dish. After leaching out PEG, the resulting membrane had small pores of ~ 2.5 μm on the air-cured surface and bigger pores of ~ 12 μm on glass-cured surface.

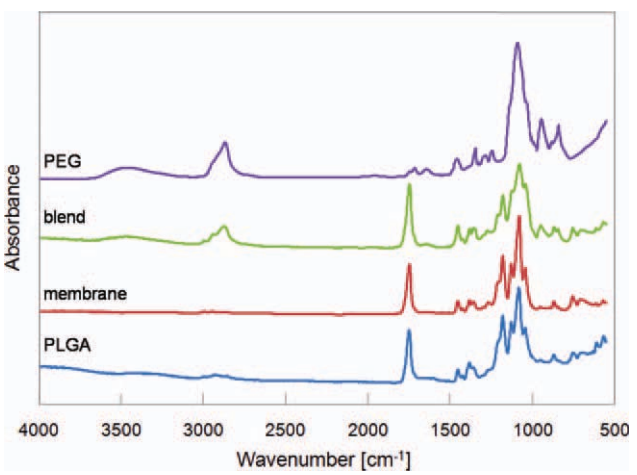

Figure 7 FTIR-ATR spectra of PEG 1000, PLGA/PEG blend, PLGA membrane, and PLGA film. [Color figure can be viewed in the online issue, which is available at wileyonlinelibrary.com.]

Controlling membranes' microstructure by PEG molecular weight

To evaluate the influence of PEG molecular weight on the microstructure of PLGA membranes, several PEGs were used at a specific concentration of 60%, which in the case of PEG 400 used as a pore former, assured the highest porosity and the best mechanical properties important from the point of view of possible medical use.

The PEG leach out percentage from each blend was close to theoretical value. Moreover, in the FTIR spectra of the membranes no bands originating from

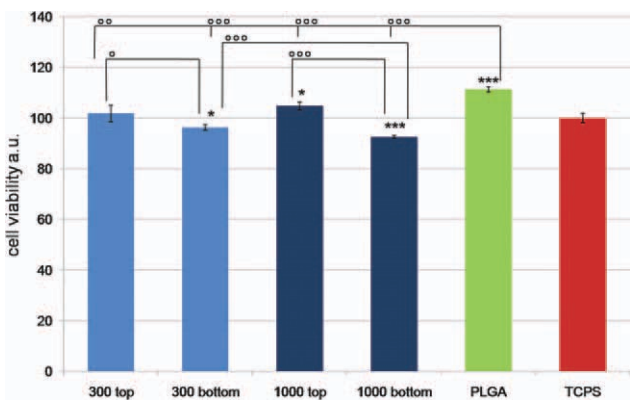

Figure 8 MG 63 cells viability (MTT assay) on PLGA membranes produced with the use of 60% PEG 300 and 1000 after 5 days of culture. Data are expressed as mean ± S.E.M. Asterisks indicate a statistical significance from the control TCPS group: $^{*}P < 0.05$; $^{***}P < 0.001$. Circles indicate a statistical significance between the groups; $^{o}P < 0.05$; $^{oo}P < 0.05$, $^{ooo}P < 0.001$. [Color figure can be viewed in the online issue, which is available at wileyonlinelibrary.com.]

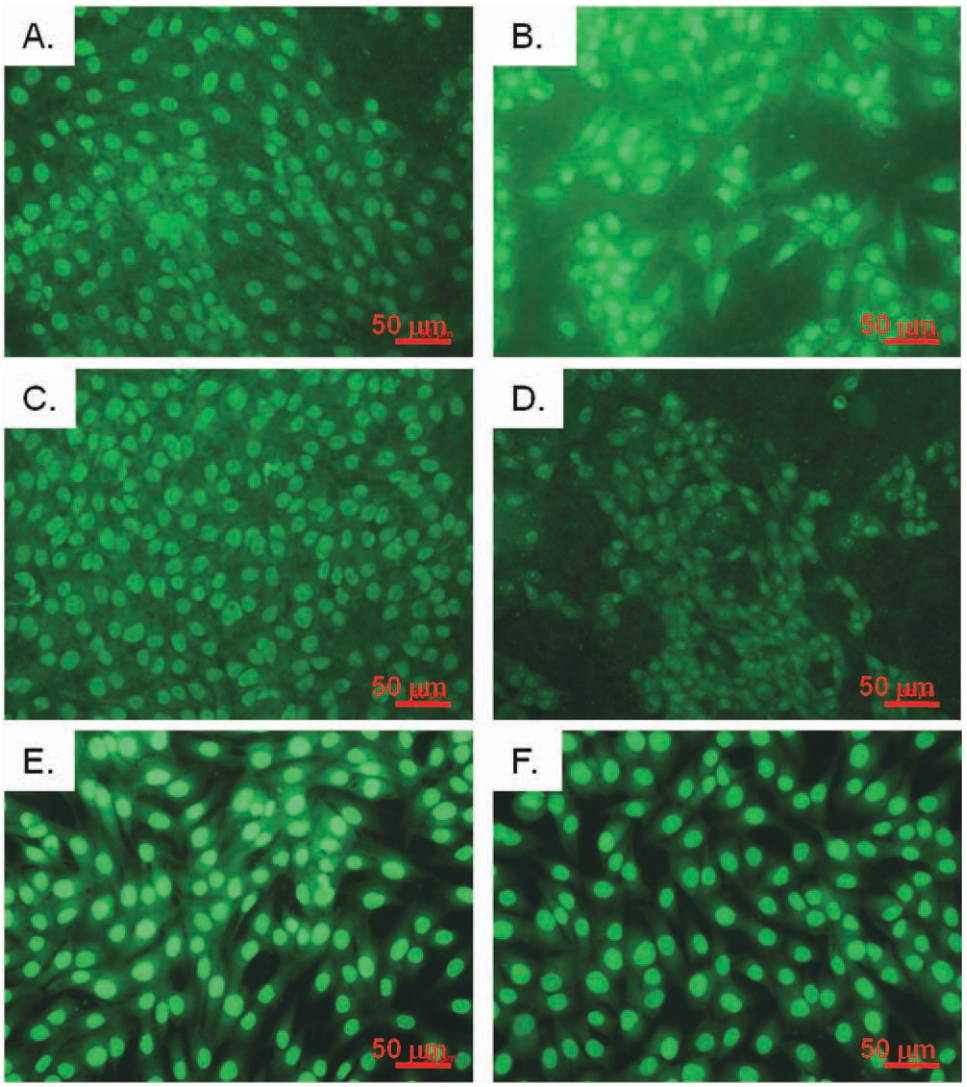

Figure 9 Morphology of MG-63 cells cultured on PLGA membranes obtained with the use of 60% PEG 300 (A,B) and PEG 1000 (C,D); top surface (A,C), bottom surface (B,D), PLGA foil (E), and reference samples TCPS (F); fluorescence staining with acridine orange and evaluation under inverted fluorescence microscope. [Color figure can be viewed in the online issue, which is available at wileyonlinelibrary.com.]

PEG were detected. It indicates that almost all of the blended PEG was dissolved in water and leached out during the washing procedure; it is also an indirect evidence of pore interconnectivity. FTIR evaluations showed that there was no chemical reaction between PLGA and PEG, however, as suggested by others hydrogen interactions cannot be excluded in this type of materials.[26]

It was found that the membranes produced with PEGs with molecular weight from 300 to 1000 Da had asymmetric microstructure: the glass-cured surface was always rougher and more porous than the air-cured surface. Moreover, porosity and size of pores on the bottom surface increased with PEG molecular weight. On the top surface, however, porosity decreased with PEG molecular weight, and when PEG molecular weight was 600 Da or more a nonporous skin was always present. The membranes produced with the use of PEG 3400 did not follow that trend.

The differences in membranes' microstructure could be explained as follows: when molecular weight of PEG is low, e.g., 300, domains rich in PEG are rather small, their number is high and they are homogenously distributed within the PLGA-rich phase. During drying solvent evaporated preferably from the PLGA-rich phase and the PEG-rich domains remained trapped within the PLGA matrix. This correlates with the lower solvent evaporation rate of PEG 300 and PLGA/PEG 300 mixtures and the highest value of remaining solvent measured after 24 h (see Table II). The membranes produced with the use of PEG 300 have small pores rather homogenously distributed on both surfaces and within the whole volume of the membranes.

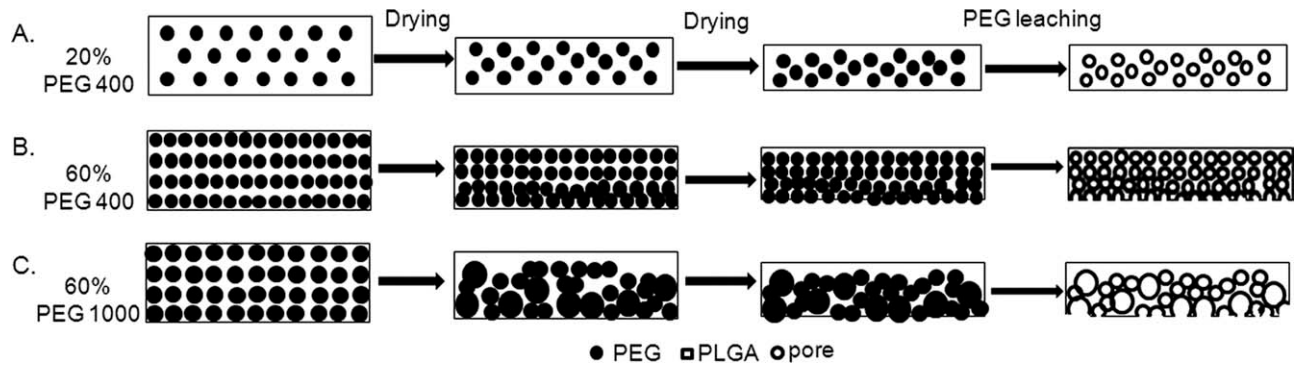

Figure 10 Diagram of the formation process of PLGA membranes by leaching out PEG from PLGA/PEG blends. A: Membranes produced with 20% PEG 400 (Small isolated PEG-rich domains are dispersed in PLGA matrix. Because solvent evaporates faster from PLGA-rich phase than from PEG-rich domains, and drying proceeds from the surface towards inside the film, PEG-rich domains are embedded into PLGA matrix. After PEG leaching out resulting membrane has small pores of size 1–2 μm quite homogenously distributed in the whole volume of the membranes). B: Membranes produced with 60% PEG 400 (Higher number of PEG-rich domains are dispersed in PLGA matrix than in situation A. At the beginning of drying some of the PEG-rich domains in the surface/subsurface regions remained trapped within the PLGA matrix. As drying proceeds PEG-rich domains inside the film start to coalesce. After leaching out of PEG, the resulting membrane has small pores of ~2.5 μm on the air-cured surface and bigger pores of ~12 μm on the glass-cured surface. C: Membranes produced with 60% PEG 1000 (Because of higher PEG molecular weight, the PEG-rich domains dispersed in PLGA matrix have a bigger size than in situation B. Due to higher solvent evaporation on the surface PLGA-rich skin is formed. Coalescence of bigger PEG-rich domains inside the film occurs. After leaching out of PEG the resulting membrane has nonporous skin on the air-cured surface and the biggest pores of ~20 μm on the glass-cured surface.

When PEGs 400, 600, and 1000 Da at the same concentration of 60% were used in production of PLGA membranes, the size of the PEG-rich domains in the blends increased with PEG molecular weight, but their number decreased. It can be attributed to a widely known tendency of decrease in solubility when molecular weight increases and a fact that the size of polymer bundles in the solvent increases with molecular weight of the polymer.[40] In these samples solvent evaporation rates were higher and the values of remaining solvent measured after 24 h were lower. As in the previous sample, at the beginning, during drying, solvent evaporated preferably from PLGA-rich phase, and because relative number of PEG-rich domains was lower, it resulted in skin formation on the air-cured surface. It also resulted in coalescence of PEG-rich domains inside the film and their preferential accumulation on the glass-cured surface. Interestingly, the size of these domains was the highest for PEG 1000. It should also be kept in mind that PEG 1000 is solid (see Fig. 6, insert) and it is more crystalline[41] than other liquid, low-molecular weight PEGs examined in this study. Proposed mechanisms of membranes' formation with the use of 60% PEG 400 and PEG 1000 are shown in Figure 10(B,C), respectively.

When PEG 3400 was used as a pore former, PLGA membrane had nonporous skin on the top surface, while on the bottom surface small irregular pores were observed. Moreover, bottom skin was delaminated, because of creation of big PEG-rich domains, which separated from the membrane after PEG was washed out. Such behavior can also be attributed to crystallization of PEG-rich domains at room temperature, or the highest degree of crystallinity of PEG 3400 (87.2%)[41] among all PEGs used in this study.

Biological properties—Compatibility with cells in culture

To verify if PLGA membranes produced were compatible with cells *in vitro*, viability and morphology of osteoblast-like cells were studied. The cells were cultured on both surfaces of two membranes produced with the use of PEG 300 and PEG 1000, and they were compared with cells cultured on reference nonporous PLGA foil and control TCPS.

It was found that cells adhere and grow on all the materials; the differences in cell viability were very small, although statistically significant. The highest cell viability, higher than on control TCPS, was measured on the nonporous PLGA foil. These results once again prove the excellent biological properties of the raw PLGA used in this study.[10,30,42] On the top surfaces of the membranes, i.e., those which were least rough and least porous, the cells viability was higher or the same as on control TCPS. On the bottom surfaces, i.e., those of the higher porosity and roughness, cells viability was significantly lower.

Microscopic observations show that the cells cultured on the top, less porous surfaces of the membranes were homogenously distributed and their morphology was similar to those on PLGA foil and TCPS. Contrarily, the cells cultured on the bottom, more porous surfaces tended to aggregate. This behaviour of

cells does not exclude the use of the materials as membranes for medical applications. On the contrary, it shows that by microstructural cues it might be possible to control biological performance of bone cells.

CONCLUSION

Typical membranes for guided tissue regeneration in periodontology have fibrous asymmetric microstructure: smoother side is aimed at contacting soft tissue and preventing fibroblasts to enter bonny defect, while the other more porous and rough side of the membrane enables osteoblasts to adhere and grow. In this study, it was shown that it is possible to obtain nonfibrous, porous, flexible, asymmetric PLGA membranes by leaching out PEG from PLGA/PEG blends of defined composition. The size and distribution of pores in the membranes depended on PEG molecular weight: low-molecular weight PEG resulted in more homogenous distribution of pores within the membrane, while high-molecular weight PEG resulted in asymmetric membranes with the skin on the air-cured surface and bigger pores on the glass-cured surface. Mechanism of phase separation and blend formation in the PLGA/PEG system depended on molecular weight and concentration of PEG as well solubility parameters and solvent evaporation rate. The membranes are compatible with osteoblast-like cells *in vitro*, have asymmetric, porous structure and their mechanical properties offer good surgical handiness.

The authors thank P. Dobrzynski (Centre of Polymer and Carbon Materials, Polish Academy of Sciences, Zabrze, Poland) for synthesizing polymer used in this work, K. Pielichowska (AGH-UST, Department of Biomaterials, Krakow, Poland) for fruitful discussions, and T. Douglas (Radboud University Nijmegen, The Netherlands) for careful reading of the manuscript.

References

1. Stamatialis, D. F.; Papenburg, B. J.; Gironés, M.; Saiful, S.; Bettahalli, S. N. M.; Schmitmeier, S.; Wessling, M. J Membr Sci 2008, 308, 1.
2. Ulbricht, M. Polymer 2006, 47, 2217.
3. Alpar, B.; Leyhausen, G.; Günay, H.; Geurtsen, W. Clin Oral Invest 2000, 4, 219.
4. Yang, F.; Both, S. K.; Yang, X.; Walboomers, X. F.; Jansen, J. A. Acta Biomater 2009, 5, 3295.
5. Kikuchi, M.; Koyama, Y.; Yamada, T.; Imamura, Y.; Okada, T.; Shirahama, N.; Akita, K.; Takakuda, K.; Tanaka, J. Biomaterials 2004, 25, 5979.
6. Stavropoulos, A.; Sculean, A.; Karring, T. Clin Oral Invest 2004, 8, 226.
7. Nieminen, T.; Kallela, I.; Keränen, J.; Hiidenheimo, I.; Kainulainen, H.; Wuolijoki, E.; Rantala, I. Int J Oral Max Surg 2006, 35, 727.
8. Xianmiao, C.; Yubao, L.; Yi, Z.; Li, Z.; Jidong, L.; Huanan, W. Mater Sci Eng 2009, 29, 29.
9. Seyednejad, H.; Ghassemi, A. H.; van Nostrum, C. F.; Vermonden, T.; Hennink, W. E. J Controlled Release 2011, 152, 168.
10. Pamula, E.; Filova, E.; Bacakova, L.; Lisa, V.; Adamczyk, D. J Biomed Mater Res 2009, 89, 432.
11. Owen, G. R.; Jackson, J.; Chehroudi, B.; Burt, H.; Brunette, D. M. Biomaterials 2005, 26, 7477.
12. Naira, L. S.; Laurencin, C. T. Prog Polym Sci 2007, 32, 762.
13. Houchin, M. L.; Topp, E. M. J Appl Polym Sci 2009, 114, 2848.
14. Ho, M.-H.; Hsieh, C.-C.; Hsiao, S.-W.; Thien, D. V. H. Carbohydr Polym 2010, 79, 955.
15. Park, Y. J.; Nam, K. H.; Ha, S. J.; Pai, C. M.; Chung, C. P.; Lee, S. J. J Controlled Release 1997, 43, 151.
16. Kim, K. H.; Jeong, L.; Park, H. N.; Shin, S. Y.; Park, W. H.; Lee, S. C.; Kim, T. I.; Park, Y. J.; Seol, Y. J.; Lee, Y. M.; Ku, Y.; Rhyu, I. C.; Han, S. B.; Chung, C. P. J Biotechnol 2005, 120, 327.
17. Cima, L. G.; Vacanti, J. P.; Vacanti, C.; Ingber, D.; Mooney, D.; Langer R. J Biomech Eng 1991, 113, 143.
18. Moriya, A.; Maruyama, Y.; Ohmukai, Y.; Sotani, T.; Matsuyama, H. J Membr Sci 2009, 342, 307.
19. Kim, J. K.; Taki, K.; Nagamine, S.; Ohshima, M. J Appl Polym Sci 2009, 111, 2518.
20. Song, S. W.; Torkelson, J. M. J Membr Sci 1995, 98, 209.
21. Mao, Y.; Zhou, J.; Cai, J.; Zhang, L. J Membr Sci 2006, 279, 246.
22. Tsuji, H.; Horikawa, G. Polym Int 2007, 56, 258.
23. Kim, W. K.; Char, K.; Kim, C. K. J Polym Sci Part B: Polym Phys 2000, 38, 3042.
24. Nakane, K.; Hata, Y.; Morita, K.; Ogihara, T.; Ogata, N. J Appl Polym Sci 2004, 94, 965.
25. Tsuji, H.; Smith, R.; Bonfield, W.; Ikada, Y. J Appl Polym Sci 2000, 75, 629.
26. Lin, W. J.; Lu, C. H. J Membr Sci 2002, 198, 109.
27. Selvam, S.; Chang, W. V.; Nakamura, T.; Thomas, P. B.; Trousdale, M. D.; Mircheff, A. K.; Schechter, J. E.; Yiu, S. C. Tissue Eng Part C: Methods 2009, 15, 463.
28. Dobrzynski, P.; Kasperczyk, J.; Janeczek, H.; Bero, M. Macromolecules 2001, 34, 5090.
29. Pamula, E.; Blazewicz, S.; Krok, M.; Koscielniak, D.; Dobrzynski, P. Polish Pat. P-391519 (2010).
30. Pamula, E.; Dobrzynski, P.; Szot, B.; Kreter, M.; Krawciow, J.; Plytycz, B.; Chadzinska, M. J Biomed Mater Res A 2008, 87, 24.
31. Pielichowska, K.; Gkowinkowski, S.; Lekki, J.; Binias, D.; Pielichowski, K.; Jenczyk, J. Eur Polym J 2008, 44, 3344.
32. Pamula, E.; Blazewicz, M.; Paluszkiewicz, C.; Dobrzynski, P. J Mol Struct 2001, 596, 69.
33. Pan, S. X.; Li, Y.; Feng, H. L.; Bai, W.; Gu, Y. Y. Mater Sci Eng C 2006, 26, 724.
34. Li, J.; Zuo, Y.; Cheng, X.; Yang, W.; Wang, H.; Li, Y. J Mater Sci: Mater Med 2009, 20, 1031.
35. Ignatius, A. A.; Ohnmacht, M.; Claes, L. E.; Kreidler, J.; Palm, F. J Biomed Mater Res 2001, 58, 564.
36. Schenderlein, S.; Luck, M.; Muller, B. W. Int J Pharm 2004, 286, 19.
37. Sepassi, K.; Yalkowsky, S. H. J Pharm Sci Technol 2006, 7, E1.
38. Iijima, H.; Iwata, M.; Inamoto, M.; Kamide, K. Polym J 1997, 29, 147.
39. Kamide, K.; Iijima, H.; Matsuda, S. Polym J 1993, 25, 1113.
40. Sperling, L. H. Introduction to Physical Polymer Science, 3rd ed.; Wiley: New Jersey, 2006.
41. Pielichowski, K.; Flejtuch, K. Polym Adv Technol 2002, 13, 690.
42. Pamula, E.; Bacakova, L.; Filova, E.; Buczynska, J.; Dobrzynski, P.; Noskova, L.; Grausova, G. J Mater Sci: Mater Med 2008, 19, 425.